Molecular Computations for Understanding Crystallization Pathways for Amorphous Calcium Carbonate

Srishti Kar, YSP Student, *Belmont High School*
Soumalya Chatterjee, YSP Student, *Sharon High School*
Mentor: Moneesh Upmanyu, Department of Mechanical & Industrial Engineering, *Northeastern University*

Northeastern University College of Engineering
Northeastern University Michael B. Silevitch and Claire J. Duggan Center for STEM Education

Abstract

The focus of this study is on amorphous calcium carbonate (ACC). The overarching goal for this project is to study the structure and stability of ACC, and the mechanisms associated with its crystallization. We used computational modeling based on calcium-ion interactions to stabilize ACC and explored a combination of pair-wise intermolecular interactions to understand the origin of the amorphous structure. Our goal was to understand more about this mechanism: What conditions cause it? Can ACC exist as a metastable structure, and not just as an ephemeral prerequisite for crystalline Calcium Carbonate ($CaCO_3$)? How can we replicate this mechanism using molecular dynamic (MD) simulations?

Background

Unit Cells

Unit cells are the smallest repeating unit of a crystalline structure. Its atomic arrangement can determine the properties of a material.

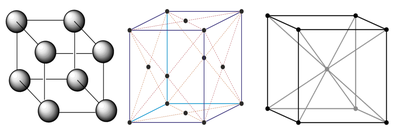

Simple Cubic (SC) | Face-Centered Cubic (FCC) | Body-Centered Cubic (BCC)

Atomic Packing Factor

Atomic Packing Factor is a measure of how efficiently atoms condense and arrange themselves within a given unit cell.

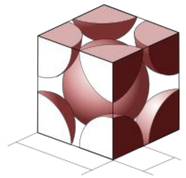

$$APF = \frac{N_{atoms} V_{atom}}{V_{unit\ cell}}$$

$APF_{SC} = 0.52$
$APF_{FCC} = 0.68$
$APF_{BCC} = 0.74$

Real-World Applications

The focus of this study is on amorphous calcium carbonate (ACC). It is the intermediate for crystallization - the arrangement of atoms into an organized formation - and also important for:

- **Carbon sequestration:** A series of methods combating harmful greenhouse gas emissions that exacerbate climate change.
- **Biomineralization:** One of many such methods include a mechanism adopted by marine life to form shells, bones, exoskeletons, and beyond. See these chemical mechanisms to understand:
  Greenhouse gas → Carbonic Acid: $CO_2 + H_2O \rightarrow H_2CO_3$
  Dissociation of Carbonic Acid: $H_2CO_3 \rightarrow H^+ + HCO_3^-$
  Dissociation of Ion: $HCO_3^- \rightarrow H^+ + CO_3^{2-}$
  Crystallization of Calcium Carbonate: $Ca^{2+} + CO_3^{2-} \rightarrow CaCO_3$
- **Sustainable materials:** Can be used to develop next generation technologies such as cements and more.
  Examples: Eggshells, seashells, limestone, marble, pearls, coral

Figure 1: Samples of $CaCO_3$ in the forms of (from left to right) crystal, pearl, powder, shell, and limestone

Methods

Simulation tools: Used LAMMPS, a classical MD simulation engine, run on Northeastern University's Explorer supercomputing cluster in MobaXterm, in tandem with OVITO, a 3D molecular visualization tool, for visual feedback and analysis.

Simulation method: Performed molecular computations using Newton's classical equations of motion, with time integration via time discretization.

Crystalline vs. amorphous identification: Used the radial distribution function (RDF) tool in OVITO to analyze density-versus-radius curves.

- Well-defined spikes indicate a crystalline structure.
- A flatter curve indicates an amorphous structure.

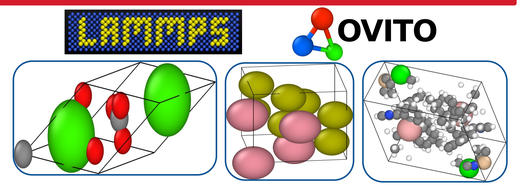

Figure 2: Unit cells of $CaCO_3$ variations (in order) Calcite, Aragonite, and Vaterite in OVITO

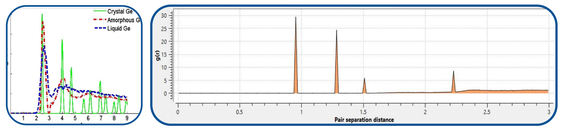

Figure 3: left (a) - RDF of Germanium in different states of matter; right (b) - sample RDF curve in OVITO

Interaction potentials: Studied Lennard-Jones (LJ) and Lennard-Jones-Gauss (LJG) energy curves.

- For LJ-Gauss, calculated the resulting double wells and varied input values in the Gaussian term (circled) to observe changes in the curve.

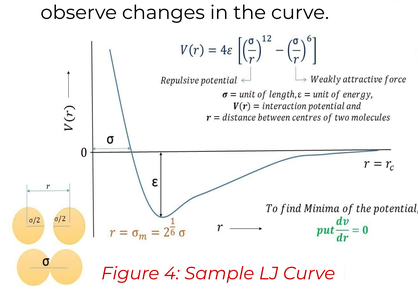

Figure 4: Sample LJ Curve

$$V(r) = 4\epsilon\left[\left(\frac{\sigma}{r}\right)^{12} - \left(\frac{\sigma}{r}\right)^{6}\right] - C\exp\left(-\frac{(r-r_0)^2}{2w^2}\right)$$

V(r) = Total potential between energy between two particles
r = Distance between the particles
ϵ_G = Depth of Gaussian minimum
σ = Distance at which potential energy is zero
r_G = Position of the Gaussian minimum
r_{lj} = Position of the Lennard-Jones minimum
ϵ_{lj} = Depth of Lennard-Jones potential well

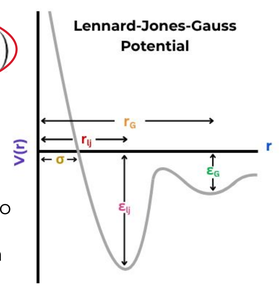

Figure 5: Sample LJG Curve

Force/motion calculations: F(x) = -dU/dx

- Used force and known mass to calculate acceleration to then determine final velocity and displacement.

Results

When we lowered the temperature, we noticed emerging crystalline clusters in figure 6b, suggesting that the sample crystallizes or stabilizes within this temperature range.

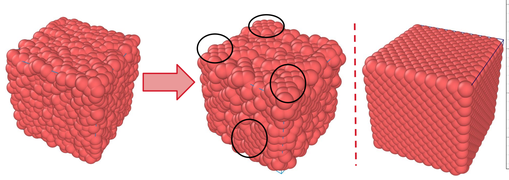

Figure 6: left (a) - Ca-Ca interactions of sample at temperature of 0.8 (arbitrary units); middle (b) - Ca-Ca interaction at temperature of 0.2, emerging FCC crystalline clusters circled; right (c) - reference crystalline sample, FCC

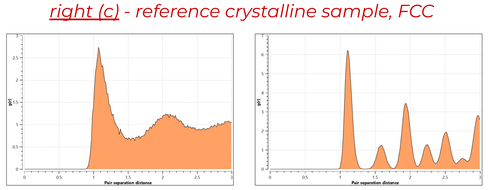

Figure 7: left (a) - RDF of sample from figure 6a; right (b) - RDF of sample from figure 6b

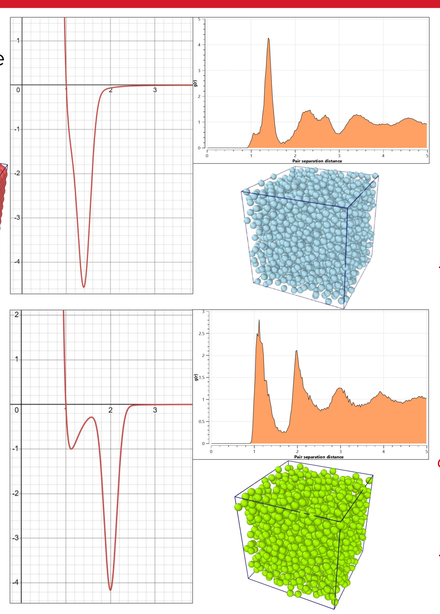

Figure 8: left (a) - Energy curve with parameters σ = 0.14, ε = 4.1, r_0 = 1.4 (arbitrary units), showing single-well curve with absolute minimum at x = 1.4 ; upper right (b) - RDF of sample, peaking at a distance of 1.4; lower right (c) - sample of Ca-Ca interactions

Figure 9: left (a) - Energy curve with parameters σ = 0.14, ε = 4.1, r_0 = 2.0, showing a double-well curve with local minima at x = 1.1 and x = 2.0; upper right (b) - RDF of sample, peaking at a distance of around 1.1 and 2.0; lower right (c) - sample of Ca-Ca interactions

Conclusion and Future Steps

When performing our molecular simulations by focusing on coarse-grained Ca-Ca interactions, we showed that the amorphous structure arises from the multiple wells in the Lennard-Jones-Gauss binding energy curves. In other words, the stable crystalline structure was unable to form due to the geometric frustration created by the double wells.

In figure 6, we noticed that lower temperatures lead to emerging crystalline clusters. Figure 7 corroborates this further as 7a's continuous and undefined peaks indicate an amorphous structure while 7b's peaks are isolated and defined, indicating an emerging crystalline structure.

In figures 8 and 9, there is a correlation between the distance where local/absolute minima exist and the pair separation distances in the RDF functions where sharp peaks/maxima exist. For the energy curves, adjusting the σ value - and therefore the bond distance - moved the larger minima side-to-side. With this, we could make two separate minima or superpose the curves to create one deeper minima.

Through these experiments, we realized that ACC, in fact, *can* exist as a metastable structure with the correct parameters and not immediately transition into a crystalline form. Another factor to consider is the hydrated nature of ACC; the presence of water introduces new intermolecular interactions that allow ACC to retain its amorphous shape. In the future, we could explore parameters which lead to full crystallization as opposed to stable ACC forms. Additionally, we could visually incorporate carbonate ions into our simulations to imagine more realistic scenarios.

Acknowledgements

Department of Mechanical & Industrial Engineering
Moneesh Upmanyu, *Professor, MIE, NU*
Jong Seto, *Professor, Arizona State University*
Center for STEM Education
Claire Duggan, *Executive Director*
Jennifer Love, *Associate Director*
Nicolas Fuchs, *Program Manager*
Mary Howley, *Administrative Officer*
Frances Corcell, Kenneth Santizo, & Ahmed Othman, *YSP Coordinators*

References

Beniash, E., Aizenberg, J., Addadi, L., & Weiner, S. (1997). *Amorphous calcium carbonate transforms into calcite during sea urchin larval spicule growth. Proceedings of the Royal Society B: Biological Sciences, 264*(1380), 461–465. https://doi.org/10.1098/rspb.1997.0066

Kapil, V., Anelli, A., Rossi, M., Michaelides, A., & Cheng, B. (2023). *Geometrically frustrated interactions drive structural complexity in amorphous calcium carbonate. Nature Chemistry, 15*(12), 1783–1791. https://doi.org/10.1038/s41557-023-01339-2

Michel, F. M., MacDonald, J., Feng, J., Phillips, B. L., Ehm, L., Tarabrella, C., Parise, J. B., & Reeder, R. J. (2008). *Structural characteristics of synthetic amorphous calcium carbonate. Chemistry of Materials, 20*(14), 4720–4728. https://doi.org/10.1021/cm800324v

Rygel, M., & Quinton, P. (n.d.). Carbonate Precipitation. LibreTexts Geosciences. Retrieved 7 13, 2026, from https://geo.libretexts.org/Courses/SUNY_Potsdam/Sedimentary_Geology%3A_Rocks_Environments_and_Stratigraphy/06%3A_Carbonate_Sedimentary_Rocks/6.02%3A_Carbonate_Precipitation

Sun, W., Dacek, S. T., Ong, S. P., Hautier, G., Jain, A., Richards, W. D., Gamst, A. C., Persson, K. A., & Ceder, G. (2018). *Moving beyond the constraints of chemistry via crystal structure discovery with isotropic multiwell pair potentials. Proceedings of the National Academy of Sciences, 115*(42), 10686–10691. https://doi.org/10.1073/pnas.1806531115

Young Scholars Program at Northeastern University
Claire Duggan, Program Director

This work was supported by the National Science Foundation.